Supramolecular recognition: On the kinetic lability of thermodynamically stable host–guest association complexes

Andrew J. Goshe*, Ian M. Steele*, Christopher Ceccarelli†, Arnold L. Rheingold†, and B. Bosnich*§

*Department of Chemistry, University of Chicago, 5735 South Ellis Avenue, Chicago, IL 60637; and †Department of Chemistry and Biochemistry, University of Delaware, Newark, DE 19716

Edited by Jack Halpern, University of Chicago, Chicago, IL, and approved January 16, 2002 (received for review November 2, 2001)

A molecular receptor consisting of a spacer bearing two cofacially disposed terpyridyl–palladium–ligand (terpy-Pd-L) units rigidly separated by about 7 Å has been investigated for molecular recognition of planar aromatic molecules. It is found that although the receptor forms stable 1:2 host–guest association complexes with 9-methylanthracene (9-MA), the guest undergoes very rapid site exchange within the receptor and with external free 9-MA. A crystal structure of the 2:1 adduct shows one 9-MA in the molecular cleft defined by the two terpy-Pd-L units and the other resides on an outside face of one terpy-Pd-L unit. To establish the site residency time of the guests, a number of tethered molecules were prepared. These involve an anthracene molecule tethered to a pyridine ligand bound to the palladium atoms to form intramolecular host–guest adducts. Rotating-frame Overhauser effects were used to infer the site residency of the anthracene guests in the receptor. Variable-temperature ^{1}H NMR spectroscopy of the intramolecular host–guest complexes has revealed that the site residency time of the anthracene guests is 1.6×10^{-5} sec at 20°C and 1.3 sec at −90°C in acetone solution. Whereas the guests are thermodynamically stable, they are kinetically very labile. A crystal structure of one of the tethered host–guest adducts reveals the expected structure which is the same as that determined in solution by ^{1}H rotating-frame Overhauser enhancement spectroscopy experiments.

The current intense interest in supramolecular chemistry is the result of several parallel trends in chemistry. Synthetic chemistry has evolved to a stage where traditional methods can produce just about any molecule of modest size and complexity. These methods usually involve the formation of kinetically stable bonds in a predetermined sequence. The construction of each of these bonds allows for the deployment of a variety of synthetic methods that serve as alternatives in the synthetic orchestration. Although powerful, these methods have limitations when confronted with the task of producing the very large complex molecular structures that exist in biology and that are required for the development of material science. It is clear that a new, nontraditional, approach is required for the construction of structurally defined molecules that are in the nanoscale domain. To achieve this aim, inspiration is drawn from biology.

The overall structures of biology are usually the result of thermodynamically controlled self-assembly. The process requires first the construction of kinetically stable bonds between a sequence of molecular units. The relative geometries of these bonds and the substituents on the units possess all of the information required for the molecule to self-assemble into a defined structure, the properties of which are unique to the self-assembled molecule. Molecular recognition, a fundamental property of biological molecules, is manifested in the self-assembled structure. Synthetic supramolecular structures are generally formed by the principles just outlined.

Table 1 lists the types of bonds that are generally used for the construction of synthetic supramolecular structures (1). Included are the respective bond strength ranges and the kinetic lability and thermodynamic stability. There are exceptions to the entries but the data serve to indicate general trends. Covalent carbon bonds and many third row transition metal bonds are stable and nonlabile, and such bonds are used as the permanent components of supramolecular structures. These components carry the structural information that leads to thermodynamically controlled self-assembly of the final supramolecular structure. The bonds that combine the components are required to be stable but kinetically labile in order that the most stable structure is formed rapidly. Such bonds include metal–ligand and hydrogen bonds. Thus a self-assembled supramolecular structure consists of nonlabile structurally encoded fragments that are assembled by stable but labile bonds. Once formed, the supramolecular structures can act as hosts for molecular recognition. The forces that control molecular recognition are generally weaker. Recognition depends critically on the structures of both the host and guest and on the solvent environment.

Table 1. Supramolecular assembly bonds

Interactions	Energy (kcal/mole)	Stability	Lability	Illustration
Covalent Carbon Bond	40-120	High	Low	C—Y
Covalent	20-80	High	High	1st Row M-L
Coordinate		High	Medium	2nd Row M-L
Bond		High	Low	3rd Row M- L
Hydrogen Bond	1-15	Medium	High	A—H····:B

The molecular recognition interactions are listed in Table 2, where it will be noted that a range of energy interactions obtain, but in all cases the host–guest complexes are highly labile unless association and dissociation is controlled by steric impediments provided by the host (1). The interactions shown in Table 2 are well known and are illustrated in the right column. van der Waals interactions, an empirical formulation, are included in the list of interactions. The illustrations in Table 2 are largely self-explanatory, but two of these may require elaboration. Three $\pi-\pi$ stacking interactions are shown, and on the assumption that the stability is determined by dipolar interactions, the structure drawn on the right is the most stable, followed by the slipped face-to-face structure drawn at the center. The eclipsed face-to-face structure is the least stable. The stability of host–guest associations is controlled to a significant degree by the solvation energies of the host, the guest, and the host–guest association complex. Depending on the

This paper was submitted directly (Track II) to the PNAS office.

Abbreviations: 9-MA, 9-methylanthracene; ROE, rotating-frame Overhauser effect; ROESY, rotating-frame Overhauser enhancement spectroscopy; terpy, terpyridyl; py, pyridine; COSY, correlation spectroscopy.

Data deposition: Crystallographic data (excluding structure factors) for the structures in this paper have been deposited with the Cambridge Crystallographic Data Centre as supplementary publication no. CCDC 173843. These data can be obtained free of charge from www.ccdc.cam.ac.uk/conts/retrieving.html (or from the Cambridge Crystallographic Data Centre, 12, Union Road, Cambridge CB2 1EZ, U.K.; E-mail: deposit@ccdc.cam.ac.uk).

§To whom reprint requests should be addressed: E-mail: bos5@midway.uchicago.edu.

Table 2. Supramolecular recognition interactions

Interaction	Energy (kcal/mol)	Distance Dependence	Stability	Lability	Illustration
Ion-Ion	10-90	$1/r$	High	High	
Ion-Dipole	10-50	$1/r^2$, $1/r^4$ [a]	High	High	
Dipole-Dipole	1-10	$1/r^3$, $1/r^6$ [a]	Low	High	
Cation-π	1-20	$1/r^2$, $1/r^4$ [b]	Medium	High	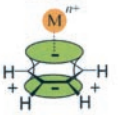
π-π stacking	1-5	$1/r^3$, $1/r^6$ [c]	Low	High	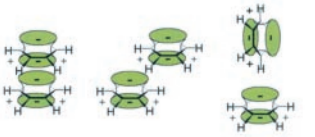
Dispersion	1-5	$1/r^6$	Low	High	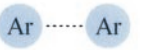
Solvent Effects [d]	1-10		High	High	

[a]The inverse distance dependence is different for a fixed ion–dipole *(1/r²)* compared to a freely rotating ion–dipole interaction *(1/r⁴)*. For dipole–dipole interactions, fixed dipoles have a *1/r³* distance dependence, whereas freely rotating dipoles vary as *1/r⁶*.
[b]Noncovalent cation–π interactions are assumed to be controlled by charge–dipole interactions *(1/r²)* and by charge-induced dipole interactions *(1/r⁴)*.
[c]π–π interactions are assumed to be controlled by fixed dipole–dipole interactions *(1/r³)*, by freely rotating dipole–dipole interactions *(1/r⁶)*, and by dispersion interactions *(1/r⁶)*.
[d]S, solvent; G, guest; H, host.

relative contributions of these solvation energies, the association constant for host–guest formation can vary dramatically from solvent to solvent. The stability of host–guest complexes may be determined as a sum of different interactions, although usually a dominant force is ascribed to the stability.

Given the data in Table 1, it is not surprising to find that an increasing emphasis on the use of metal complexes in supramolecular assembly has emerged recently (2–6). In addition to the favorable stability–lability relationship of many metal–ligand bonds, metal-based supramolecular assemblies can be varied in overall charge and, because of the variety of bond dispositions, metal complexes can provide unique supramolecular geometries. Much of the work in this area has been directed at producing interesting large structural motifs and less attention has been devoted to molecular recognition, although the work of Fujita (5, 7–9), in particular, has demonstrated that metal-based supramolecular systems can be powerful molecular receptors.

This account describes our work on the stability and lability of guest molecules associated with a host that has unique characteristics. It will be shown that, although stable host–guest complexes can be formed, they are exceptionally labile at ambient temperatures. Few comparable studies on the dynamics of host–guest association have appeared (10–12).

The Molecular Receptor

The molecular receptors consist of several parts: a spacer–(tridentate) chelator, **1**, a spacer–chelator square planar complex, **2**, and linkers, **3**, **4**, and **5**. By using appropriate spacer–chelator complexes, **2**, and the linkers, **3**, **4**, and **5**, the molecular rectangle, **6**, the trigonal prism, **7**, and the tetragonal prism, **8**, should form by thermodynamically controlled self-assembly. For these to form, a number of characteristics are required to be embodied in the spacer–chelator complex and in the linkers. The spacer–chelator complex **2** requires rigidity to reduce the degrees of freedom of the molecule. As the number of degrees of freedom is reduced, the molecule becomes more disposed to self-assemble in a particular geometry. Similarly, rigid spacers serve the same purpose. Thus, structural characteristics of the spacer–chelator complex and the linker carry the information that leads to thermodynamically controlled self-assembly by a self-correcting process. For rapid self-assembly, the ligand, L, in **2** must be a good leaving group and the metal-linker bonds must also be kinetically labile. The lability of metal-ligand bonds depends principally on the nature of the metal and to some extent on the characteristics of the ligand.

The spacer–chelator complexes discussed here are of the type **9**, the preparation of which is described elsewhere (13). The fully

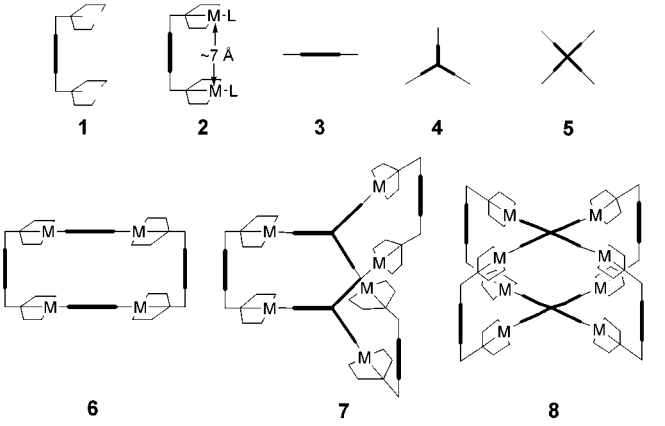

oxidized spacer as well as other metal complexes have been prepared. The molecule **9** has a number of characteristics that were expected to lead to the formation of supramolecular assemblies with rigid spacers. Further, **9** was expected to act as a molecular receptor by incarcerating guests in the molecular cleft. The receptor **9** contains a rigid spacer that carries two cofacially disposed terpyridyl–palladium–ligand (terpy-Pd-L) units. These two terpy-Pd-L units are separated by about 7 Å, but this separation can be contracted to some extent while retaining a nearly eclipsed cofacial disposition by concerted rotation of these units about the chelator–spacer single bonds. The separation between the two terpy-Pd-L units is sufficient to incarcerate planar aromatic molecules and square-planar complexes, the "thickness" of which match the cavity provided by the molecular cleft.

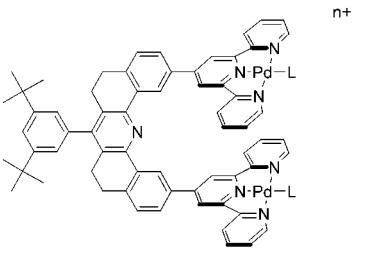

9

When L is a good leaving group, such as CH_3CN, addition of the linkers **10** or **11** to **9** leads to the molecular rectangle **6** (14) or the trigonal prism **7** (J. D. Crowley, A.J.G., and B.B., unpublished work). The supramolecular assemblies are formed rapidly and quantitatively in acetonitrile solutions at 25°C. Although the molecular rectangle and trigonal prism act as receptors for a variety of guests, the systems, **9** [L = Cl or pyridine (py)], which have a single molecular cleft for guest incarceration are the subject of this paper.

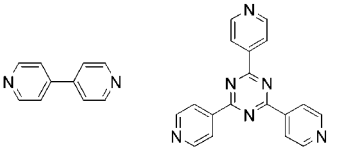

10 **11**

When dissolved in acetonitrile or acetone solutions, the receptor **9** associates with a variety of planar molecules including **12**, **13,** and **14**. Addition of solutions of the guest molecules to yellow solutions of **9** results in the immediate development of a deep red color, suggesting host–guest association. In the case of 9-methylanthracene (9-MA; **12**), its association with **9** (L = Cl) in acetonitrile solutions was measured by the ^{1}H NMR titration method at 21°C (13, 15–17). Two equilibrium (association) constants were obtained, $K_1 = 650\ M^{-1}$ and $K_2 = 250\ M^{-1}$. Whereas it is clear that one of the association constants represents the incarceration of 9-MA in the molecular cleft, it is not obvious how to ascribe the location of the second 9-MA. This multiple association appears to be a general phenomenon for 9-MA association with molecules derived from **9**. Thus, for example, the molecular rectangle **6**, derived from the linker **10**, associates with four 9-MA guests, presumably by associating two 9-MA guests for each **9** fragment.

The nature of the 2:1 complex is inferred from the extended crystal structure of the adduct (Fig. 1). The solid-state structure shows that 9-MA molecules reside in the cleft as expected, but the structure also reveals a second 9-MA molecule that stacks on the

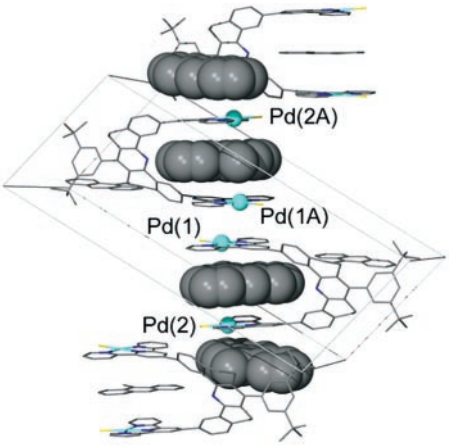

Fig. 1. An illustration of the extended structure of [**9** (L = Cl)]$^{2+}$·2(9-MA). The box is the unit cell, 9-MA molecules of the stack are shown as space-filling models, and the terpy-Pd-Cl units are shown as stick models, as are all other molecules not involved in this stack. Palladium atoms in the stack are shown as blue spheres.

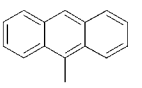

9-MA
12

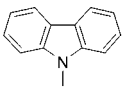

13

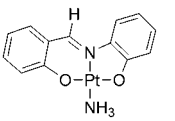

14

outer face of the terpy-Pd-Cl units. The interplanar separation between 9-MA molecules and terpy-Pd-Cl units is 3.42 Å, which is achieved by concerted rotation of the terpy-Pd-Cl units with respect to the spacer. It is probable that in solution the receptor associates with 9-MA in a similar manner, with one 9-MA inside of the cleft and the other lying on the outside face of a terpy-Pd-Cl unit. The ^{1}H NMR spectrum in the temperature range of −40°C to +70°C does not distinguish the site residency of the 9-MA units; an average ^{1}H NMR spectrum is observed, indicating that the guests are undergoing rapid interchange between sites. Fast exchange also occurs between free and associated 9-MA. Thus, although the host–guest complexes are stable, they are labile with respect to site exchange and with respect to intermolecular exchange. To ascertain the site residency time of guests, a number of new compounds were prepared.

Supporting information (26 pages) contains the experimental procedures; ^{1}H NMR, COSY, and ROESY spectra for compounds **15**, **16**, and **17**; and the crystallographic experimental section, a table of crystal data, and views for [**17**]$(PF_6)_4$. This material is available on the PNAS web site, www.pnas.org.

Dynamics of Host–Guest Complexes

The dynamic behavior of host–guest complexes was studied by temperature variation of the ^{1}H NMR spectra of the complexes **15**, **16,** and **17**, which, in the cases of **16** and **17**, are drawn with the anthracene groups in their anticipated sites. The pyridine-linked anthracene ligand required some care in design to ensure a proper unencumbered fit of the anthracene group into the molecular cleft. As noted previously, the anthracene associates with the receptor by occupying the cleft and an external terpy-Pd-L face. Thus, the anthracene groups in **16** and **17** are expected to interchange intramolecularly between these sites and it may be possible to measure the rate of interchange by temperature-dependent ^{1}H NMR spectroscopy. The compound **15** was prepared as an analogue for the study of 9-MA association.

By ^{1}H NMR titration of 9-MA with **15** in $(CD_3)_2CO$ solution at 16°C it was determined that a 2:1 complex formed with association

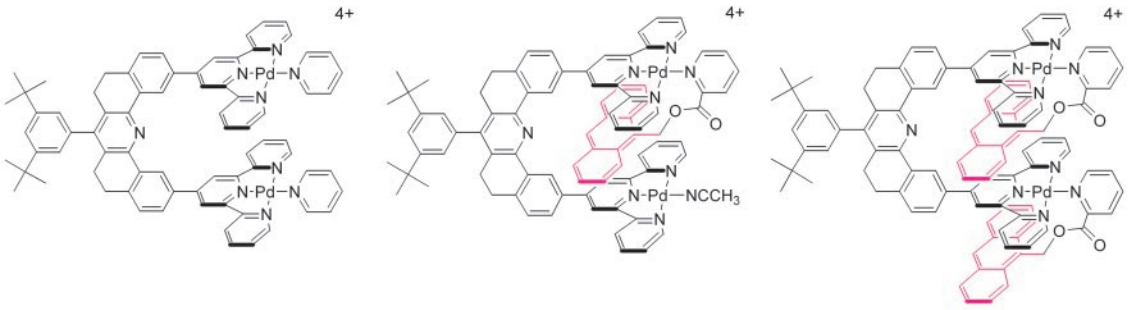

15 16 17

constants $K_1 = 400 \pm 50\ M^{-1}$ and $K_2 = 100 \pm 50\ M^{-1}$. The two 9-MA molecules of the complex are indistinguishable by ^1H NMR spectroscopy at temperatures between −90°C and 20°C, and the free and bound 9-MA molecules are indistinguishable in the same temperature range. Thus, whereas relatively stable complexes are formed, the 9-MA guest molecules exchange rapidly between their respective sites in the association complex and with free 9-MA. The site occupancies of the 9-MA guest associated with the receptor **15** have been inferred from ^1H rotating-frame Overhauser enhancement spectroscopy (ROESY), a method of measuring rotating-frame Overhauser effects (ROE) in large molecules (18–21). The ROE are informative of the relative proximity between nuclei, in this case proton nuclei. It was found that Overhauser effects existed between a number of protons of the host and those of the guests. The cross-peak Overhauser effects are consistent with the presence of a 9-MA guest in the cleft of **15** and a 9-MA guest lying on the outer faces of the terpy-Pd-py units. Further, the long axis of the 9-MA guests appears to be roughly parallel to the long axis of the terpy ligands. The cross-peak enhancements also imply that the 2:1 adducts exist as four isomers that occur by virtue of the orientations of the 9-MA methyl groups with respect to the spacer. These four isomers are represented in **18**, **19**, **20,** and **21,** where proton–proton enhancements are indicated by curved lines. Because of the rapid site exchange, the two outside faces of the terpy-Pd-Cl units are not distinguished, giving rise to ROE cross-peaks at both sites. For similar reasons, the four isomers are engaged in rapid interconversions. The ROESY experiment reflects the average population of the sites but it does provide a detailed description of the structure of 2:1 adduct. It is gratifying that the ROESY experiment provides a structure similar to that observed in the solid state for the chloro receptor (Fig. 1).

The compound **16** incorporates one tethered anthracene guest and was prepared to determine which of the two sites (in the cleft or above the terpy-Pd-L) was preferred in the 2:1 adducts. It may appear obvious that the 9-MA would prefer the cleft site, but this has not been established. Because of the lower symmetry of **16** compared with **15**, a correlation spectroscopy (COSY) experiment was performed to establish the ^1H NMR proton assignments in $(CD_3)_2CO$ solution. ROESY experiments performed on **16** in $(CD_3)_2CO$ solutions at 16°C revealed cross-peaks that indicated the anthracene guest lay exclusively in the cleft. No Overhauser effects were detected for protons that would give ROE cross-peaks if the anthracene occupied the outside terpy-Pd-L face as was observed for the 2:1 adduct of the receptor **15**. The ROESY experiments indicate the structure **22** where the cross-peaks are shown as before.

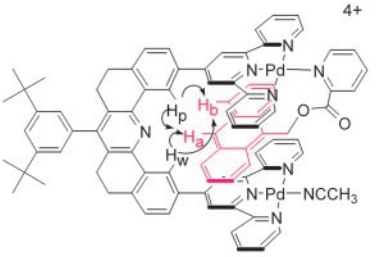

22

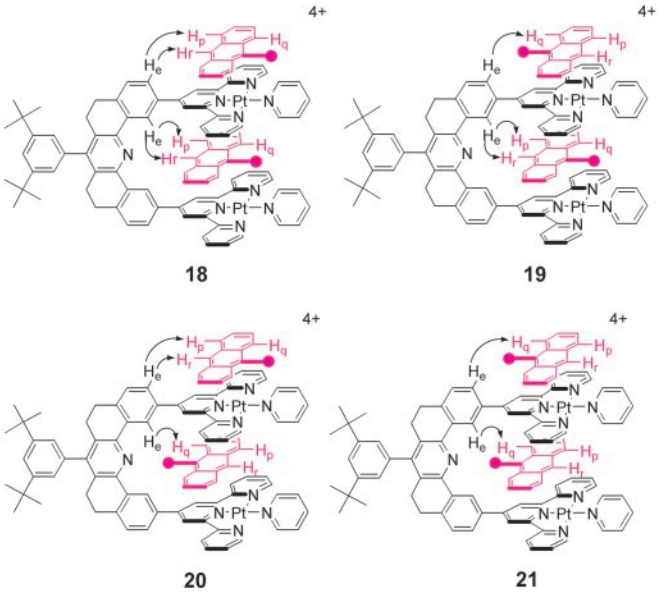

18 19 20 21

When the temperature was lowered incrementally from 20°C to −90°C no changes in the ^1H NMR spectrum of **16** were observed that would indicate that more than one site was populated by the anthracene guest. This result, however, does not necessarily imply that the anthracene group is not engaging in fluxional exchange between the inside and outside sites because, if the anthracene guest resides overwhelmingly in the cleft, its population at the outside site will not be detected. Compound **17** is a tethered analogue of **15** and it is expected that one anthracene guest will lie in the cleft and the other will reside on the outside face of the terpy-Pd-L units. This system is expected to engage in intramolecular site exchange. Given that the anthracene guest is tethered, it might be expected that the site exchange would be slower than in the case of the 2:1 9-MA adduct of **15**, which is devoid of the tether steric encumbrances. The ^1H NMR spectrum of **17** at 16°C in $(CD_3)_2CO$ solutions displays signals that indicate a symmetrical molecule, indicating that all of the sites are equally populated by the anthracene guests. This observation suggests that the two anthracene fragments are in rapid

exchange between the accessible sites. This process is intramolecular because addition of the ligand to acetone solutions of **17** provides an ^{1}H NMR spectrum at 16°C that reveals signals for both the free and bound ligands, indicating that the time scale for intramolecular site exchange is much faster than intermolecular site exchange. Further, the ^{1}H NMR spectrum is invariant to dilution in the range of 10^{-3} M to 10^{-5} M, indicating that the anthracene guest engages in intramolecular rather than intermolecular association. COSY and ROESY spectra were measured on **17** in acetone solution at 16°C to assign the signals and to infer the structure of **17**, respectively. The ROESY spectrum indicates that the expected structure, **23**, obtains and, further, that ROE cross-peaks are present at all three possible sites, which is consistent with the ^{1}H NMR spectrum.

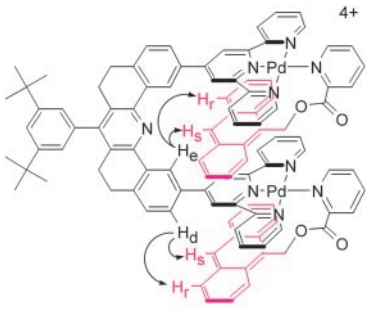

23

The ^{1}H NMR spectrum of **17** was measured in 10°C intervals between 20°C and −90°C in $(CD_3)_2CO$ solution. Temperature-dependent chemical shifts are observed for the protons and many of the signals overlap, but there are three well separated signals that are sharp at 20°C and become broad as the temperature is lowered, and at −90°C each separates into sharp signals. This latter behavior is characteristic of fluxional site exchange. These data can be processed by conventional methods to provide the activation free energy, $\Delta G^{\ddagger}$, and the corresponding enthalpy, $\Delta H^{\ddagger}$, and entropy, $\Delta S^{\ddagger}$, and, of course, the rate constants and site residency life-times for the fluxional site exchange (22–24).

Using any of three signals that undergo coalescence and separation, we found that $\Delta G^{\ddagger} = 10.1$ kcal/mol, $\Delta H^{\ddagger} = 8.23$ kcal/mol, and $\Delta S^{\ddagger} = -8.47$ cal/mol·K for the site exchange process. The average site residency time (life-time) of the guests in any site configuration is 1.6×10^{-5} sec at 20°C and 1.3 sec at −90°C.

The mechanism of site exchange is consistent with the process **17** ⇌ **24** ⇌ **25,** where the intermediate **24** is produced by stepwise (intramolecular) dissociation of the anthracene fragments from their respective sites while maintaining Pd–N connectivity. Such a process, **17** ⇌ **25**, requires the rotation of the pyridine ligands, which could conceivably be encumbered by the terpy ligands. There appears to be a little steric hindrance to pyridine ligand rotation, because it was found that these ligands freely rotate at −90°C in **15**. That the fluxional site exchange represents the process **17** ⇌ **25** is supported by the observation that the proton signal at $\delta = 9.15$ ppm splits into two signals at −90°C. These signals refer to the inner two protons of the spacer (protons e, structure **23**), and the appearance of two signals at −90°C indicates an unsymmetrical molecule consistent with structure **17**. The molecule **17** could exist in two interconverting forms by flipping of the spacer between the racemic and meso forms arising from the conformations of the two reduced rings. This interconversion in analogous molecules is a very low energy process that would not be apparent in the temperature span of the present study (25, 26). A possible method of interconverting from **17** to **25** is by locked rotation of terpy-Pd-L units, but it has been demonstrated that rotation of large aromatic molecules in

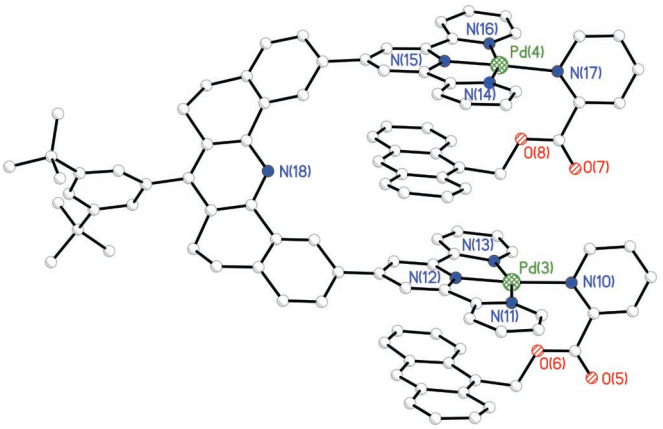

Fig. 2. A ball-and-stick representation of a ''side'' view for one of the molecules in the unit cell of **17.** Counter ions and solvent molecules have been removed for clarity.

place of the terpy-Pd-L substituents is a higher energy process than the one observed here even in the absence of a guest in the molecular cleft (26, 27). Thus, the mechanism of site exchange is most likely that illustrated in outline by the sequence **17** ⇌ **24** ⇌ **25**.

Crystal Structure

Isolation of crystals suitable for x-ray diffraction of **17** proved difficult, but eventually crystals that provided useful data were obtained by vapor diffusion of methanol into a methyl ethyl ketone solution of the PF_6^- salt. The crystals formed as **17** $(PF_6)_4$·2Et(Me)CO. The solid-state structure is shown in Figs. 2 and 3, where it will be seen that the expected structure obtains. Two molecules exist in the unit cell and each molecule is in the same absolute configuration. The bond lengths and bond angles are unexceptional. Each of the molecules in the unit cell has slightly different structural parameters and, in what follows, average values are given. The interplanar separations are shown in the two-dimensional illustration of the structure **26**. The interplanar angles, defined by the mean plane of the anthracene unit and the mean plane of the terpy ligand, are shown in brackets in **26**. The

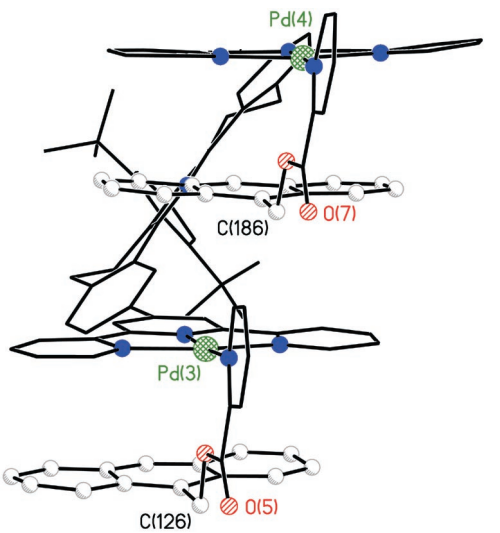

Fig. 3. A ball-and-stick representation of a ''front'' view for one of the molecules in the unit cell of **17.** Counter ions and solvent molecules have been removed for clarity.

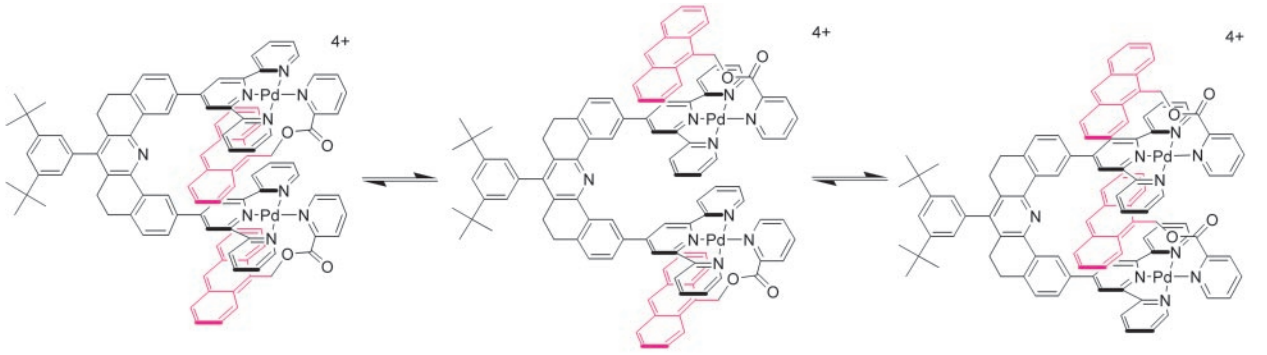

17 24 25

interplanar separations are those expected for π-stacked aromatic molecules, and each stacking unit is aligned roughly parallel to the other, as required. It is gratifying to note that the crystal structure is similar to that inferred from ROESY experiments in solution and that the structure is similar to the one in Fig. 1, which contains untethered anthracene guests. To achieve the interplanar separations necessary for π–π stacking, the terpy-Pd-L units engage in concerted rotation to decrease the interplanar separations of the two terpy-Pd-L units to 6.84 Å. Consequently, the terpy-Pd-L planes are not perpendicular to the mean molecular plane of the spacer, giving the molecule a twisted configuration (Fig. 3). The ability of the receptor to adjust the interplanar separation of the cleft is an important factor in stabilizing the guest.

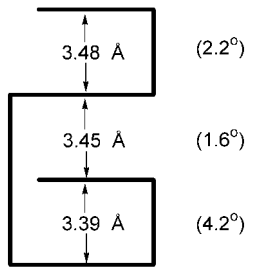

26

The extended solid-state structure of **17** is shown in Fig. 4, where infinite alternate stacking of anthracene and terpy-Pd-L units is observed. This structure is similar to, but different from, that observed for the structure shown in Fig. 1. The latter exists as units of eight stacks, which includes terpy-Pd-Cl–terpy-Pd-Cl stacking, whereas the former displays infinite alternate anthracene–terpy-Pd-L stacking.

Discussion

The work described here demonstrates a number of features of molecular recognition. Perhaps the most significant is the observation that whereas host–guest complexes can be thermodynamically stable, they, at the same time, can be exceeding labile kinetically. The forces that control host–guest formation in the present study probably involve attractive π–π interactions and may also involve charge-induced-dipole attraction between the positively charged terpy-Pd-L units and the π electrons of the anthracene guests (Table 2). Because these forces attenuate rapidly with distance, particularly if, as is probable, the dipolar interactions are not fixed, the interplanar separation of the receptor is crucial in obtaining stable host–guest association complexes. As noted, the receptor described here is able to adjust this separation with minimum energy cost.

The solution stability of host–guest complexes depends on solvation effects (Table 2), and it is interesting in this regard that one of the anthracene guests resides on the outer face of a terpy-Pd-L unit in solution. Given that the solid-state structures show extensive stacking of units, it is perhaps surprising that greater aggregation is not observed in solution. This may be because of the low concentration ($\approx 10^{-3}$ M) at which the studies were carried out. For other guests, however, solution gels are formed, indicating extensive association, perhaps resembling that observed in the solid state.

As noted earlier, molecular recognition is a subtle phenomenon, which depends on weak interactions, and it is difficult to describe the stability of a host–guest complex in terms of a single dominant interaction. The stability usually depends on the additive effects of multiple weak interactions which, in concert, provide the molecular recognition. One of the challenges in chemistry in the near future is to understand and deploy these weak noncovalent interactions, not only for molecular recogni-

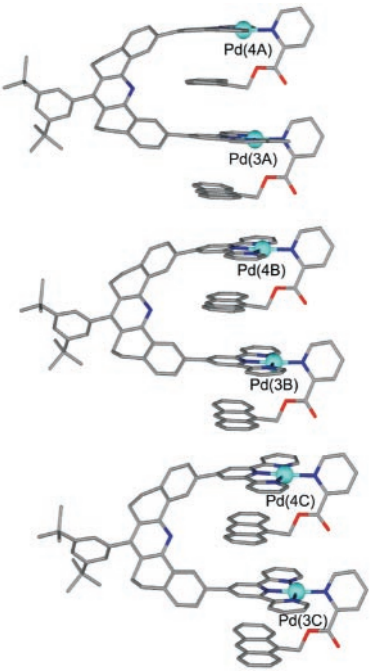

Fig. 4. An illustration of a "side" view of three molecules of **17** that belong to an infinite stack of molecules in the crystal of $[\mathbf{17}]^{4+}$. Counter ions and solvent molecules have been removed for clarity.

tion but also for the construction of large molecules in the nanoscale domain.

This work was supported by grants from the Basic Sciences Division of the Department of Energy.

1. Goshe, A. J., Crowley, J. D. & Bosnich, B. (2001) *Helv. Chim. Acta* **84,** 2971–2985.
2. Leininger, S., Olenyuk, B. & Stang, P. J. (2000) *Chem. Rev.* **100,** 853–908.
3. Swiegers, G. F. & Malefetse, T. J. (2000) *Chem. Rev.* **100,** 3483–3537.
4. Jones, C. J. (1998) *Chem. Soc. Rev.* **27,** 289–299.
5. Biradha, K. & Fujita, M. (2000) in *Advances in Supramolecular Chemistry*, ed. Gokel, G. W. (JAI Press, Stamford, CT), pp. 1–39.
6. Caulder, D. L. & Raymond, K. N. (1999) *J. Chem. Soc. Dalton Trans.,* 1185–1200.
7. Fujita, M. (1999) *Acc. Chem. Res.* **32,** 53–61.
8. Fujita, M. (1998) *Chem. Soc. Rev.* **27,** 417–425.
9. Fujita, M. & Ogura, K. (1996) *Coord. Chem. Rev.* **148,** 249–264.
10. Garel, L., Dutasta, J.-M. & Collet, A. (1993) *Angew. Chem. Int. Ed. Eng.* **32,** 1169–1171.
11. Brotin, T., Lesage, A., Emsley, L. & Collet, A. (2000) *J. Am. Chem. Soc.* **122,** 1171–1174.
12. Ballardini, R., Balzani, V., Credi, A., Brown, C. L., Gillard, R. E., Montalti, M., Philp, D., Stoddart, J. F., Venturi, M., White, A. J. P., *et al*. (1997) *J. Am. Chem. Soc.* **119,** 12503–12513.
13. Sommer, R. D., Rheingold, A. L., Goshe, A. J. & Bosnich, B. (2001) *J. Am Chem. Soc.* **123,** 3940–3952.
14. Goshe, A. J. & Bosnich, B. (2001) *Synlett,* 941–944.
15. Kneeland, D. M., Ariga, K., Lynch, V. M., Huang, C.-Y. & Anslyn, E. V. (1993) *J. Am. Chem. Soc.* **115,** 10042–10055.
16. Schneider, H.-J. & Yatsimirsky, A. K. (2000) *Principles and Methods in Supramolecular Chemistry* (Wiley, Chichester, U.K.), pp. 137–190.
17. Tsukube, H., Furuta, H., Odani, A., Takeda, Y., Yoshihiro, K., Inoue, Y., Liu, Y., Sakamoto, H. & Kimura, K. (1996) in *Comprehensive Supramolecular Chemistry,* eds. Davies, S. E. D. & Ripmeester, J. A. (Pergamon, Oxford), Vol. 8**,** pp. 426–481.
18. Neuhaus, D. & Williamson, M. P. (2000) *The Nuclear Overhauser Effect in Structural and Conformational Analysis* (Wiley, New York), 2nd Ed.
19. Schneider, H.-J. & Yatsimirsky, A. K. (2000) *Principles and Methods in Supramolecular Chemistry* (Wiley, Chichester, U.K.), pp. 230–240.
20. Klärner, F.-G. Burkert, U., Kamieth, M., Boese, R. & Benet-Buchholz, J. (1999) *Chem. Eur. J.* **5,** 1700–1707.
21. Mo, H. & Pochapsky, T. C. (1997) *Prog. Nucl. Magn. Reson. Spectrosc.* **30,** 1–38.
22. Petrucci, S., Eyring, E. M. & Konya, G. (1996) in *Comprehensive Supramolecular Chemistry,* eds. Davies, S. E. D. & Ripmeester, J. A. (Pergamon, Oxford), Vol. 8**,** pp. 483–497.
23. Schneider, H.-J. & Yatsimirsky, A. K. (2000) *Principles and Methods in Supramolecular Chemistry* (Wiley, Chichester, U.K.), pp. 259–263.
24. Binsch, G. (1968) in *Topics in Stereochemistry*, eds. Eliel, E. L & Allinger, N. L. (Interscience, New York), Vol. 3**,** pp. 97–185.
25. Rabideau, P. W. (1989) in *The Conformational Analysis of Cyclohexanes, Cyclohexadienes, and Related Hydroaromatic Compounds* (VCH, New York), pp. 81–88.
26. Zimmerman, S. C. (1993) in *Topics in Current Chemistry*, ed. Weber, E. (Springer, Berlin), Vol. 165, pp. 72–101.
27. Zimmerman, S. C., VanZyl, C. M. & Hamilton, G. S. (1989) *J. Am. Chem. Soc.* **111,** 1373–1381.